Wanderlust Kinetics and Variable Ca^{2+}-Sensitivity of *Drosophila*, a Large Conductance Ca^{2+}-Activated K^+ Channel, Expressed in Oocytes

Shai D. Silberberg,* Armando Lagrutta,‡ John P. Adelman,‡ and Karl L. Magleby§

*Department of Life Sciences, Ben Gurion University of the Negev, Beer-Sheva 84105, Israel; ‡Vollum Institute, Oregon Health Sciences University, Portland, Oregon 97201 USA; and §Department of Physiology and Biophysics, University of Miami School of Medicine, Miami, Florida 33101 USA

ABSTRACT Cloned large conductance Ca^{2+}-activated K^+ channels (BK or maxi-K^+ channels) from *Drosophila* (*dSlo*) were expressed in *Xenopus* oocytes and studied in excised membrane patches with the patch-clamp technique. Both a natural variant and a mutant that eliminated a putative cyclic AMP-dependent protein kinase phosphorylation site exhibited large, slow fluctuations in open probability with time. These fluctuations, termed "wanderlust kinetics," occurred with a time course of tens of seconds to minutes and had kinetic properties inconsistent with simple gating models. Wanderlust kinetics was still observed in the presence of 5 mM caffeine or 50 nM thapsigargin, or when the Ca^{2+} buffering capacity of the solution was increased by the addition of 5 mM HEDTA, suggesting that the wanderlust kinetics did not arise from Ca^{2+} release from caffeine and thapsigargin sensitive internal stores in the excised patch. The slow changes in kinetics associated with wanderlust kinetics could be generated with a discrete-state Markov model with transitions among three or more kinetic modes with different levels of open probability. To average out the wanderlust kinetics, large amounts of data were analyzed and demonstrated up to a threefold difference in the $[Ca^{2+}]_i$ required for an open probability of 0.5 among channels expressed from the same injected mRNA. These findings indicate that cloned *dSlo* channels in excised patches from *Xenopus* oocytes can exhibit large variability in gating properties, both within a single channel and among channels.

INTRODUCTION

Large-conductance Ca^{2+}-activated K^+ channels (BK or maxi-K^+ channels) are found in a wide variety of tissues (Marty, 1981; Pallotta et al., 1981; Latorre et al., 1982; Adams et al., 1982; Rudy, 1988; Latorre et al., 1989). These channels, which typically have a conductance of 150–350 pS in symmetrical 150 mM KCl, are activated by micromolar concentrations of Ca^{2+} at the inner membrane surface, $Ca^{2+}{}_i$, and increase their open probability with depolarization. Although considerable progress has been made toward characterizing the gating properties of BK channels, headway has been slowed by the fact that different channels from the same cell type can display large differences in Ca^{2+}-dependent properties (McManus and Magleby, 1991; Wu et al., 1996). Such differences may arise from different primary structures of the channels. It is known that the same tissue can express several different types of Ca^{2+}-activated K^+ channels (Farley and Rudy, 1988), and recent cloning of the BK channel suggests that alternative splicing could give rise to a large family of functionally diverse channels (Atkinson et al., 1991; Adelman et al., 1992; Butler et al., 1993; Lagrutta et al., 1994; Pallanck and Ganetzky, 1994; Tseng-Crank et al., 1994; Wei et al., 1994).

If the variability arises mainly from different alternative splicings, then the variability should be decreased or eliminated when cloned channels of the same type are examined. In this paper we study one of the alternatively spliced variants (A1/C2/E1/G3/I0) of *dSlo*, the cloned BK channel from *Drosophila* (Atkinson et al., 1991; Adelman et al., 1992), and a mutated form of this channel in which serine is changed to alanine (S942A) to eliminate a putative PKA phosphorylation site (Esguerra et al., 1994). Differences in the $[Ca^{2+}]_i$ for half-maximum activation for both wild-type and S942A channels expressed in *Xenopus* oocytes are still present. In addition, we find that both wild-type and S942A channels typically display large, slow fluctuating changes in open probability (P_o). These slow changes, termed "wanderlust kinetics," have a time course that varies from seconds to minutes. They are too large to be accounted for by the expected stochastic variation from a simple kinetic model, but could be accounted for by a kinetic model that allows transitions among three or more modes with different levels of P_o. In contrast to more typical mode shifting for BK channels that reflects changes in both open and shut interval durations, wanderlust kinetics was mainly associated with shifts in shut interval durations. Increasing the buffering capacity of the intracellular solution with HEDTA buffer had little effect on the wanderlust kinetics, which was still observed after treatment with caffeine or thapsigargin, two agents that would be expected to deplete possible intracellular Ca^{2+} stores in the excised patch. A preliminary report of some of these observations has appeared (Silberberg et al., 1995).

Received for publication 20 October 1995 and in final form 11 March 1996.

Address reprint requests to Dr. Karl L. Magleby, Ph.D., Department of Physiology and Biophysics, University of Miami School of Medicine, P.O. Box 016430, Miami, FL 33101-6430. Tel.: 305-243-6236; Fax: 305-243-6898; E-mail: kmagleby@mednet.med.miami.edu.

0006-3495/96/06/2640/12 $2.00

MATERIALS AND METHODS

Expression of channels in *Xenopus* oocytes

Xenopus oocytes were enzymatically separated using collagenase as previously described (Dahl, 1992). Oocytes were injected with either mRNA transcribed in vitro from cDNA coding for variant A1/C2/E1/G3/I0 of the

dSlo Ca^{2+}-activated potassium channel (BK channel) from *Drosophila* (wild-type channel) (Adelman et al., 1992), or with mRNA in which a putative cyclic AMP-dependent protein kinase (PKA) phosphorylation site of the wild-type channel was inactivated by replacing serine at position 942 with alanine (S942A channel). The S942A mutant was constructed by oligonucleotide-directed mutagenesis, as described for the pAlter system (Promega). The mutation was checked by sequencing the plasmid across the mutagenesis target region, using a modification of the dideoxy sequencing method (Sequenase reagents from United States Biochemical Corp., Cleveland, OH). Single-channel currents through expressed BK channels could be recorded in excised patches of membrane within 2–4 days after injecting 2 to 10 ng of mRNA.

Single-channel recording

Currents from single BK channels were recorded from inside-out membrane patches excised from the animal pole of the injected oocytes using the patch-clamp technique (Hamill et al., 1981; Sakmann and Neher, 1995). The vitelline membrane was removed with forceps from the oocytes just before the experiments. Patch pipettes were fabricated from borosilicate glass (Sutter instruments) and coated with Sylgard 184 (Dow Corning Corp.). The tip of the patch pipette with the attached excised patch of membrane containing a single BK channel was inserted into a microchamber, which was then slightly elevated above the solution level in the oocyte dish (Barrett et al., 1982). Experimental solutions were introduced through the microchamber using a gravity-fed perfusion system and were changed via six-way rotary Teflon valves (Rheodyne, Inc.).

The pipette solution (extracellular solution) typically contained (mM): K-gluconate, 154; KCl, 6; $CaCl_2$, 1; $MgCl_2$, 1; TES buffer (*N*-Tris (hydroxymethyl)methyl-2-aminoethane sulphonic acid), 5. In a few experiments to examine the effect of low concentrations of divalent cations in the pipette solution, the pipette contained, when indicated, K-gluconate, 140 mM; KCl, 10 mM; EGTA, 1 mM; and TES, 5 mM. For most experiments the microchamber (intracellular) solution contained (mM): K-gluconate, 150; KCl, 10; TES buffer, 5; and sufficient $CaCl_2$ to achieve the desired levels of free calcium. Solutions were adjusted to pH 7.0. The buffering capacity of gluconate for Ca^{2+} was estimated by using a calcium-sensitive electrode (Corning model 476041). The voltages measured with the calcium electrode in either standard solutions and in K^+-gluconate solutions were plotted against the log [Ca^{2+}]. An apparent stability constant of 1.61 M^{-1} for Ca^{2+}-gluconate was estimated from the shift of the K^+-gluconate curve relative to the standard curve. This value was then used to calculate the amount of $CaCl_2$ needed to obtain a particular free [Ca^{2+}].

In a few experiments (where indicated), the Ca^{2+} buffering capacity of the intracellular solution was increased by adding the Ca^{2+} buffer HEDTA (*N*-(2-hydrosyethyl)-ethylenediamine-*N,N',N'*-triacetic acid). These solutions contained (mM): K-gluconate, 140; KCl, 10; TES buffer, 5; HEDTA, 5; and sufficient $CaCl_2$ to achieve the desired levels of free calcium. The HEDTA was titrated to pH 7.0 with KOH before addition, and then the final solution was again adjusted to pH 7.0. The added Ca^{2+} and estimated free Ca^{2+} were, respectively, 3.21 mM for 6.5 μM, 3.46 mM for 8.5 μM, and 3.69 mM for 11 μM. HEDTA was used as a Ca^{2+} buffer instead of EGTA, because EGTA would be saturated with Ca^{2+} at the levels of Ca^{2+} required to activate the channel, whereas HEDTA was in the middle of its buffering range.

For those experiments in which thapsigargin was added, a stock solution of 2 mM thapsigargin was made up in dimethyl sulfoxide (DMSO). Sufficient stock solution was added for a final concentration of 50 nM thapsigargin, giving 0.0025% DMSO after the 1:40,000 dilution. Because the addition of thapsigargin together with the small amount of DMSO appeared to have little or no effect on wanderlust kinetics, the effects of DMSO alone were not investigated. Thapsigargin and caffeine were obtained from Sigma.

The membrane potential of the excised patches was held at +30 mV (intracellular side positive). Current records were initially low-pass filtered at 10 kHz (−3 dB), using the integral 4-pole Bessel filter of the Axopatch 200A patch-clamp amplifier (Axon Instruments), and stored on VCR tape (DC-37 kHz) for subsequent analysis (Instrutech). Experiments were performed at room temperature (21–23°C).

Kinetic analysis of channel activity

Single-channel current records were transferred from the VCR tape to a Pentium computer at a sampling rate of 200 kHz using a Digidata 1200 interface board and pClamp 6.0 software in continuous mode (Axon Instruments). The effective low-pass filtering for the analysis, taking into account the filtering from all components, including any additional filtering, was 6.5 kHz for the experiments in Fig. 4, *B–D*, and 8.95 kHz for all of the remaining experiments. This filtering resulted in dead times of 27.5 μs and 20 μs, respectively, where dead time is the duration of a rectangular pulse that reaches 50% of its true amplitude after filtering (Colquhoun and Sigworth, 1995). All digitized current records were visually inspected for artifacts and for drifts in the baseline, both on the computer screen and from laserjet printouts of the current records at a number of different time resolutions. Data with noisy or drifting baseline current were rejected. In some cases there were occasional very brief biphasic spike artifacts that were identified visually and removed from the current records before further analysis by replacing the current values during the spike with current values equal to the average value preceding and following the spike.

After the current records were visually inspected, the durations of the open and shut intervals were measured with half-amplitude threshold analysis, as detailed by McManus and Magleby (1989). Stability plots of the interval durations, which plot the mean open and shut interval against interval number (McManus and Magleby, 1988), were then constructed to facilitate the search for moding and gating to subconductance states that may have been missed in the visual examination of the records. Transitions to the buzz and brief open mode (McManus and Magleby, 1988) and occasional gating to subconductance levels near the 50% level were readily apparent in the stability plots as step changes in the mean open times. Such atypical gating in the stability plots was checked against the current records and removed from further analysis. In general, less than about 2% of the current record in any experiment was excluded in this manner. In some experiments channel activity at high and low open probabilities was identified from visual examination of plots of open probability, P_o, against time and selected for separate analysis.

The methods used to log bin the intervals into dwell time distributions, fit the distributions with sums of exponentials using maximum likelihood fitting techniques (intervals less than two dead times were excluded from the fitting), determine the number of significant exponential components with the likelihood ratio test, estimate the most likely rate constants for discrete state kinetic models by maximum likelihood fitting of the distributions of open and shut interval durations with Q-Matrix methods, and generate simulated current records with filtering and noise have been described previously (Blatz and Magleby, 1986a,b; McManus et al., 1987; McManus and Magleby, 1988, 1991; Colquhoun and Sigworth, 1995). Dwell-time distributions are plotted with the Sigworth and Sine (1987) transformation, as the square root of the number of intervals per bin, where the bin width increases logarithmically with time without correction for the increase in bin width. A kinetic model was assumed to describe the data as well as theoretically possible if the likelihood for the description of the dwell-time distributions by the kinetic model was the same as the likelihood for the description of the dwell-time distributions for fitting sums of exponentials with all free parameters (Blatz and Magleby, 1986b).

RESULTS

Slow gating processes in *dSlo* BK channels

Experiments were performed on dSlo A1/C2/E1/G3/I0 channels (wild type) expressed in *Xenopus* oocytes and on mutated *dSlo* channels in which a putative phosphorylation site on the channels (Esguerra et al., 1994) was eliminated

by replacing the serine residue at position 942 with an alanine (S942A). As observed previously (Adelman et al., 1992), the channels in excised patches of membrane were K^+ selective, activated by micromolar concentrations of $Ca^{2+}{}_i$ and modulated by voltage, as expected for BK channels. Surprisingly, inspection of single-channel data records collected from the cloned channels over many minutes during constant experimental conditions typically indicated large and fluctuating changes in channel activity with time, and this was the case for both the wild-type and S942A channels. An example of such an experiment for a S942A channel is shown in Fig. 1, where upward current steps indicate channel opening.

The slow fluctuation between high and low channel activity is evident in Fig. 1 *A*, which presents consecutive single-channel current traces for nine continuous minutes of recording. Low activity was associated with an increasing fraction of longer duration shut intervals (Fig. 1 *B2*) when compared to high activity (Fig. 1 *B1*). The kinetics during the bursts of high and low activity appeared relatively similar (Fig. 1 *Ca* versus 1 *Cb*). Gating to a subconductance level of about 40% of the normal open level during an 11-s stretch of time is also apparent in Fig. 1 *A* (bracket near 3, Fig. 1, *B3* and *Cc*). Gating among multiple subconductance levels, although not obvious in Fig. 1, was also observed occasionally for BK channels in other patches.

In this experiment with symmetrical 160 mM K^+ (gluconate was the major anion) and a membrane potential of +30 mV, the 6.8-pA currents gave a conductance of 227 pS. Single-channel measurements of conductance for 11 channels that were studied extensively gave 227 ± 13 (SD) pA for the S942A channels (n = 6), and 230 ± 13 pA for the wild-type channels (n = 5), consistent with the expected conductance for the alternatively spliced variant with an A1 box (Lagrutta et al., 1994). Fig. 2 *A* presents a stability plot (Blatz and Magleby, 1986b) from the record in Fig. 1 *A* after excluding the data during the gating to the subconductance level. The mean open time for averages of 500 consecutive open intervals remained relatively constant during the 614,564 intervals, whereas there were large changes in the mean shut time. The changes in P_o are plotted in Fig. 2 *B* as a function of the number of intervals (20,000 intervals per point, moving average), and in Fig. 2 *C* as a function of time (10 s for each point). P_o ranged from 0.082 to 0.87 and fluctuated with a slow time course of tens of seconds to minutes (Fig. 2 *C*).

Before the start of the record in Fig. 1 *A*, there was 42.5 min of recording from the excised patch, during which there were five solution changes to different $[Ca^{2+}]_i$. Large, slow fluctuations in P_o were also present during this time. Large, slow fluctuations in P_o were also observed in 19 of 23 additional channels studied at several different $[Ca^{2+}]_i$. An example is shown in Fig. 3 *A* for a wild-type channel. Large, slow fluctuations were also observed in three out of three additional experiments in which the pipette solution contained 1 mM EGTA and no added Ca^{2+}, to reduce extracellular Ca^{2+} to low levels.

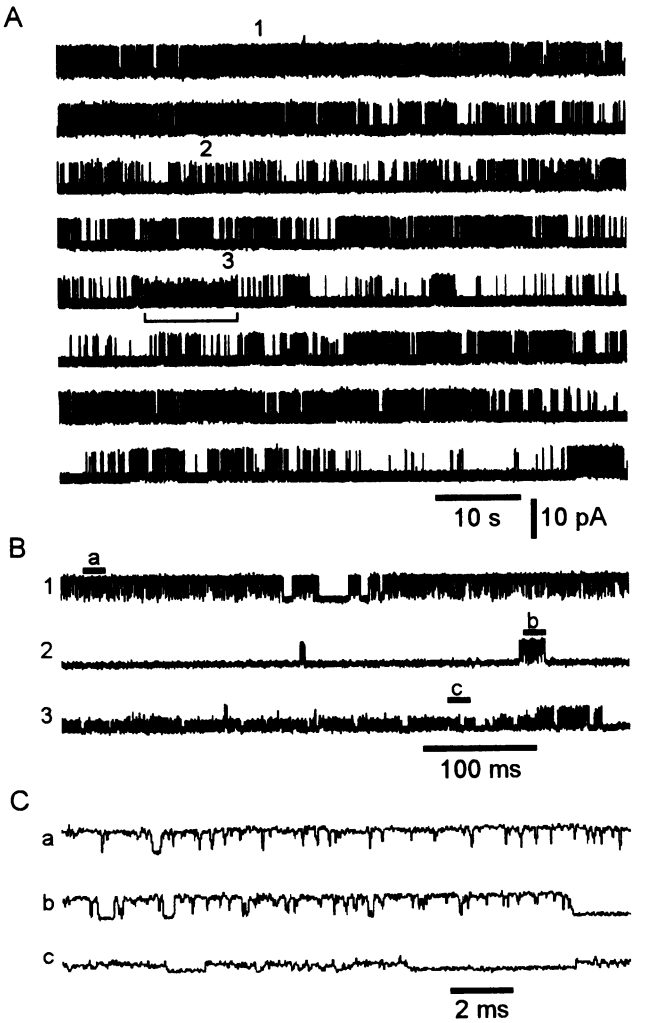

FIGURE 1 Currents recorded from a single mutated (S942A) *dSlo* BK channel. (*A*) A continuous 9-min current record from a single channel in an excised patch of membrane has been cut into eight consecutive segments for display. Upward (outward) currents indicate channel opening. Holding potential of +30 mV. 6.5 μM $Ca^{2+}{}_i$ (at the cytoplasmic face of the membrane). (*B*) Excerpts of current records from *A* presented on an expanded time scale showing high channel activity (*trace 1*), low channel activity (*trace 2*), and openings to a subconductance level (*trace 3*). The numbers to the left of the current traces correspond to the labeling in *A*. (*C*) The regions labeled *a*, *b*, and *c* in *B* are further expanded in time. The apparent bit noise in the current records reflects the resolution of the monitor used to display and plot the data, and not the resolution used for the analysis, which was considerably higher.

In three of the four channels in which P_o appeared relatively stable, the durations of recording were limited to a few minutes, so that there may not have been sufficient time for large fluctuations to become evident. For the remaining channel, P_o appeared relatively stable for one 10-min stretch out of 30 min of recording.

The wandering of the channel in the P_o domain, as shown in Figs. 1–3, suggests the term "wanderlust kinetics" to describe the phenomenon.

The large, slow fluctuations that characterize wanderlust kinetics are typically not seen for recordings from native

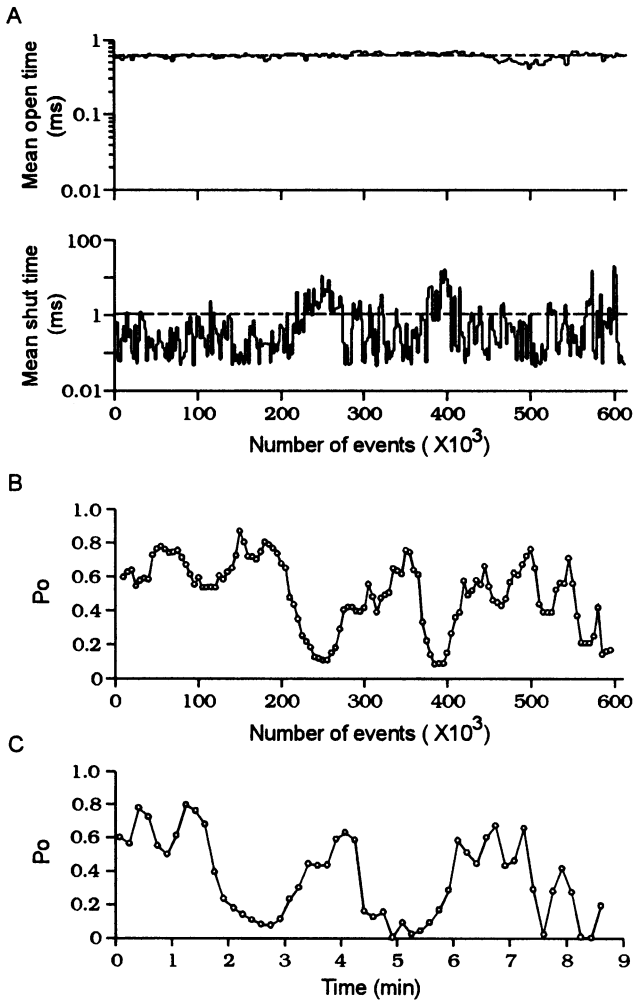

FIGURE 2 Slow variations in activity from a S942A channel. (*A*) Stability plots of the mean open and mean shut times for the current record shown in Fig. 1 *A*. Each bin in the plot represents the average duration of 500 consecutive open or shut intervals. Transitions to the brief open and buzz modes (McManus and Magleby, 1988) and to the subconductance level shown in Fig. 1 *A3* were excluded from the records before making the stability plots. This exclusion removed about 4% of the detected intervals in this experiment: 1.2% to the brief open and buzz modes and 2.8% to the subconductance level. Mean interval durations over the entire data set are shown by the dashed lines. (*B*) Fluctuations in mean channel open probability (P_o) as a function of consecutive interval number. Each point represents the average P_o of 20,000 consecutive open and shut intervals and is shifted 5,000 intervals with respect to the previous point (moving bin average). (*C*) Fluctuations in P_o as a function of time. Each point represents the P_o calculated for 10 consecutive seconds of channel activity.

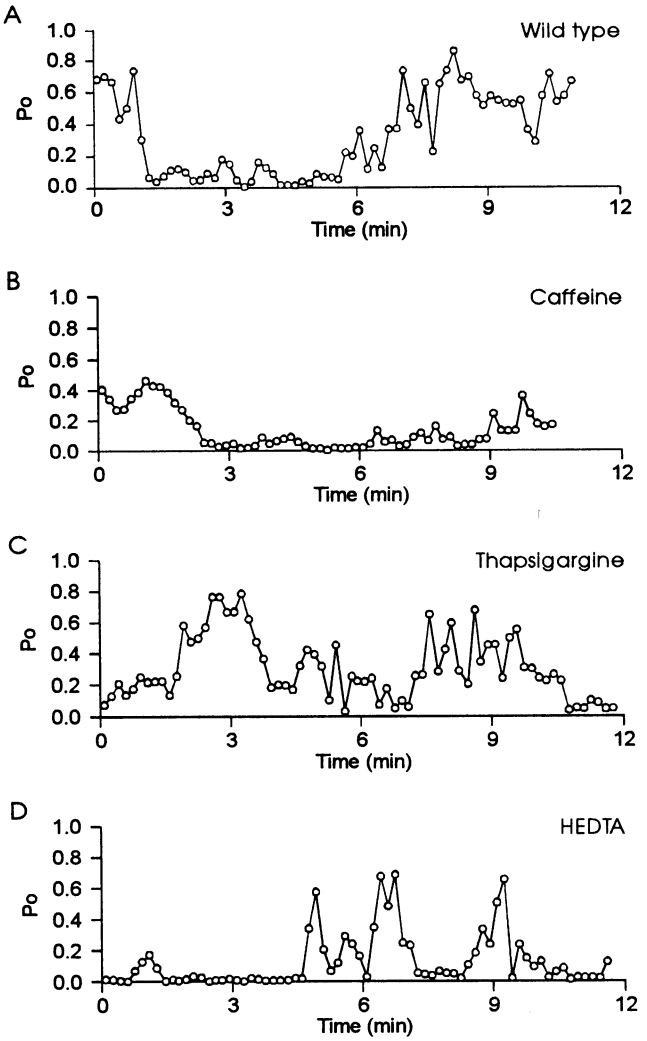

FIGURE 3 Examples of wanderlust kinetics for four BK channels. Each point plots the P_o calculated for 10 consecutive seconds of channel activity. (*A*) Slow changes in P_o for recordings from a wild-type BK channel with 8.5 μM $Ca^{2+}{}_i$. (*B*, *C*, and *D*) Slow changes in P_o for single mutant channels (S942A) in three different excised patches of membrane. For *B* there was 5 mM caffeine and 11 μM $Ca^{2+}{}_i$. The caffeine was applied 3 min before the start of the record. For *C* there was 50 nM thapsigargin (see Materials and Methods) and 8.5 μM $Ca^{2+}{}_i$. For *D* there was 5 mM HEDTA buffer and sufficient added Ca^{2+} to bring the free $Ca^{2+}{}_i$ to 11 μM. The excised patch had been exposed to HEDTA buffer for 23 min before the record in *D* was obtained.

BK channels from cultured rat skeletal muscle, either with EGTA to buffer the $Ca^{2+}{}_i$ (McManus and Magleby, 1988) or without Ca^{2+} buffers (Rothberg and Magleby, unpublished observations).

Wanderlust kinetics persist in the presence of caffeine, thapsigargin, and HEDTA

Large slow fluctuations in the activity of BK channels in large excised inside-out patches of membrane from smooth muscle cells have been associated with the release of Ca^{2+} from internal stores (Xiong et al., 1992). The fluctuations in activity were observed when the Ca^{2+}-buffering capacity of the solution at the intracellular surface was negligible and were abolished when the solution contained either 4 mM EGTA to increase the Ca^{2+} buffering capacity or 5 mM caffeine to dump Ca^{2+} from the intracellular stores. A fluctuating response was possible because the solutions contained ATP to power the Ca^{2+} pumps to refill the stores after the periodic releases of Ca^{2+}. It seems unlikely that the observed wanderlust kinetics in our experiments were due to periodic release of Ca^{2+} from internal stores in the

excised patch, because our solutions did not contain the ATP required for refilling the stores and the pipettes were small, with resistances greater than 10 MΩ. Nevertheless, we investigated the possibility of Ca^{2+} release from internal stores.

Wanderlust kinetics was still observed in six of seven excised patches in which the $Ca^{2+}{}_i$ buffering capacity of the solution at the intracellular surface was increased with the addition of 5 mM (HEDTA) (see Materials and Methods). An example of wanderlust kinetics with HEDTA is shown in Fig. 3 *D*. In this experiment the average P_o was low so that the wanderlust kinetics typically increased from the lower P_o. In other experiments with HEDTA in which the average P_o was higher, the wanderlust kinetics was similar to that shown in Fig. 3, *A* and *B*.

As a further test of whether wanderlust kinetics might be due to Ca^{2+} release from internal stores, we recorded single-channel currents from excised patches in the presence of 5 mM caffeine or 50 nM thapsigargin. Caffeine releases Ca^{2+} from internal stores (Rousseau et al., 1988) and can suppress Ca^{2+}-dependent chloride current fluctuations in *Xenopus* oocytes (Poledna and Packova, 1994). Thapsigargin inhibits the microsomal Ca^{2+} ion pump (Clapham, 1995).

Wanderlust kinetics was still observed in the three excised patches examined with 5 mM caffeine and in the five excised patches examined with thapsigargin, as shown by the examples in Fig. 3, *B* and *C*. The absolute variation in P_o in caffeine was less than for the other examples in Fig. 3 because the average P_o for this experiment before and after caffeine application was less than for the other presented experiments. The lack of effect of either increased Ca^{2+} buffering capacity or of agents that result in a depletion of Ca^{2+} from internal stores suggests that wanderlust kinetics in our experiments was not due to release of Ca^{2+} from caffeine and thapsigargin sensitive internal stores.

Expressed cloned channels display variable Ca^{2+} sensitivity

In spite of the wanderlust kinetics, it should still be possible to determine whether there are differences in Ca^{2+} sensitivity among individual cloned channels, as is the case among individual native channels in skeletal muscle (McManus and Magleby, 1991), if sufficient data are analyzed to average out the variation in P_o due to wanderlust kinetics. Fig. 4, *A* and *B*, show changes in channel activity as the $[Ca^{2+}]_i$ is decreased from 30 to 5 μM (*left arrow*) and then raised from 5 to 11 μM (*right arrow*). Fig. 4 *C* presents dose-response curves for four separate channels. Each of the points plots the average P_o for 3–16 min of data to average out the wanderlust kinetics. (Examples of the range of P_o for some of the plotted data points are given in the legend to Fig. 4.) It is readily apparent that $[Ca^{2+}]_i$ for a P_o of 0.5 varied as much as threefold among the four channels. Data from the three channels (plotted with filled symbols) were obtained on the same day from oocytes isolated from the same animal and injected with mRNA from the same batch, using experimental solutions drawn from the same premixed reservoirs. Thus, it is unlikely that the variability reflects different experimental conditions. These results suggest that either factors other than differences in primary structure, such as coupling to endogenous proteins, or modifications to the primary structure, such as phosphorylation,

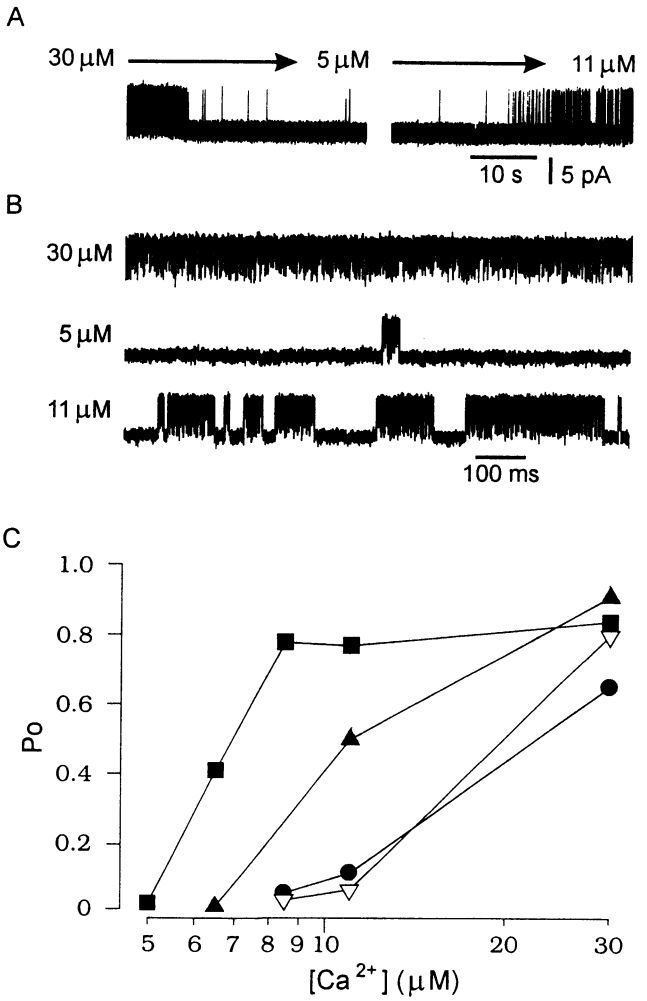

FIGURE 4 Differences in Ca^{2+} sensitivity among channels. (*A*) Changes in wild-type channel activity induced by changing $[Ca^{2+}]_i$ from 30 to 5 μM and then from 5 to 11 μM. The solutions were changing during the arrows. Upward currents indicate channel opening. (*B*) Expanded view of the records shown in *A*. (*C*) Average P_o as a function of $[Ca^{2+}]_i$ for four separate S942A channels. Each plotted symbol represents the average P_o calculated from 3–16 min of data to average out the wanderlust kinetics. For example, for the filled circle at 11 μM $Ca^{2+}{}_i$ the duration of the current record was 429 s, the mean P_o during the current record was 0.12, and the range in P_o when the current record was analyzed 10 s at a time was 0.035–0.45. For the filled triangle at 11 μM $Ca^{2+}{}_i$, the duration of the current record was 232 s, the mean P_o was 0.55, and the range in P_o was 0.29–0.76. For the filled square at 11 μM $Ca^{2+}{}_i$, the duration of the current record was 239 s, the mean P_o was 0.77, and the range in P_o was 0.66–0.87. Data from three of the four excised patches (*filled symbols*) were obtained on the same day, drawing solutions from the same reservoirs.

account for the variability (see Discussion). The data in Fig. 4 *C* are from S942A channels, indicating that the variability is not due to differences in PKA-induced phosphorylation of the channel at this specific site. Differences in Ca^{2+} sensitivity were also seen among cloned wild-type channels, but were not studied in detail.

Wanderlust kinetics appear inconsistent with simple gating models

Kinetic models with three or four open and five or six shut kinetic states can account for the major features of the Ca^{2+}-dependent kinetics of native BK channels in skeletal muscle (McManus and Magleby, 1988, 1989, 1991). A possible explanation for the wanderlust changes in P_o is that they may arise as a natural consequence of the stochastic variation associated with gating of discrete multistate models. To test this possibility, the durations of open and shut intervals were measured for the data in Fig. 1 *A* after excluding the obvious gating to subconductance levels. The distributions of open interval durations were described well by the sums of three significant exponential components (Fig. 5 *A*) and the shut by seven (Fig. 5 *B*). If the underlying rate constants associated with gating remain constant in time, as is the case for native BK channels (McManus and Magleby, 1989), then this would suggest a minimum of three open and seven shut kinetic states.

The distributions of open and shut intervals were then fitted with a simple kinetic model of the type consistent with the gating of native BK channels (McManus and Magleby, 1991). This model, with three open and seven shut states, is shown in Scheme I. The model gave

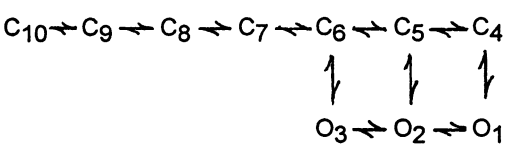

(I)

excellent descriptions of open and shut dwell time distributions (continuous lines in Fig. 5, *A* and *B*); the predicted dwell time distributions were the same as the theoretical best fit for a Markov model, in that the distributions predicted by Scheme I exactly overlapped those described by the sums of exponentials with all free parameters.

Ninety minutes of single channel data were then simulated with Scheme I using noise and filtering similar to that for the experimental data (Blatz and Magleby, 1986a; McManus et al., 1987) and analyzed to obtain P_o plots. The 9-min segment of simulated data with the greatest apparent variability was then selected and plotted in Fig. 5 *C*. The experimentally observed variability (Fig. 2 *C*) was considerably greater than the maximum variability predicted by Scheme I.

Similar results were obtained for four additional channels analyzed in this manner (two wild-type and two S942A

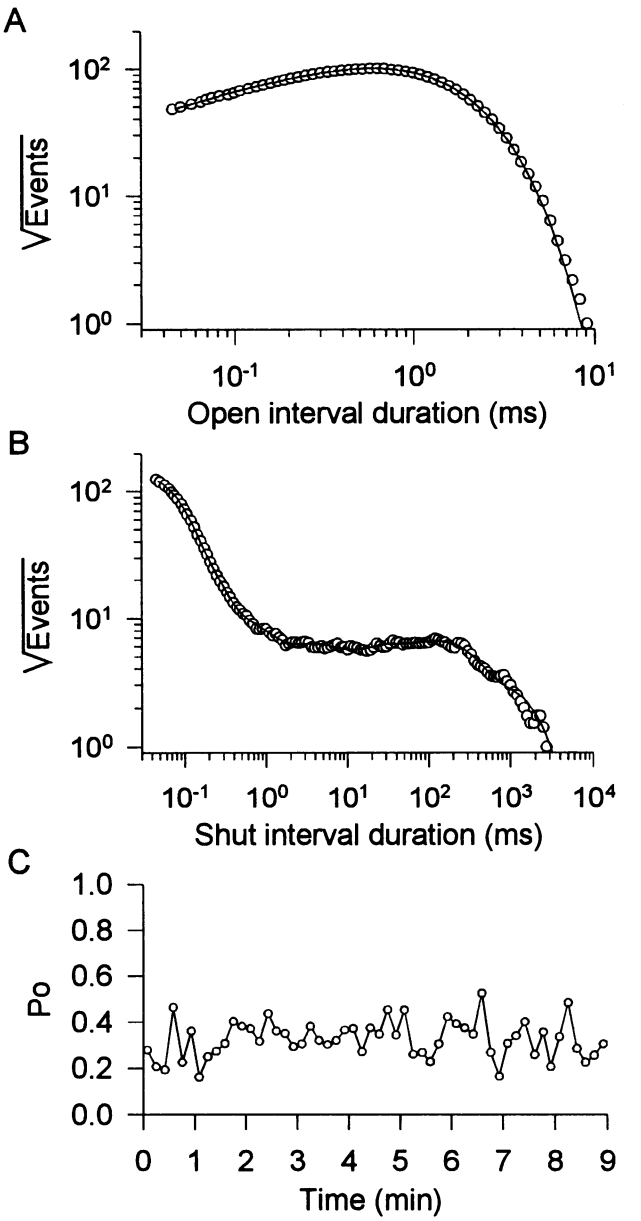

FIGURE 5 Wanderlust kinetics are complex. Distribution of open (*A*) and shut (*B*) interval durations for the data plotted in Fig. 2 *A*. The open distribution is described by the sum of three significant exponential components (*continuous line*) with time constants and (areas) of 0.068 ms (0.024), 0.42 ms (0.24), and 0.67 ms (0.74). The shut distribution is described by the sum of seven exponential components (*continuous line*) with time constants and (areas) of 0.027 ms (0.93), 0.074 ms (0.062), 0.36 ms (0.0048), 2.7 ms (0.0016), 18 ms (0.0011), 120 ms (0.0022) and 660 ms (0.00047). (*C*) Predicted variation in P_o as a function of time for Scheme I using rate constants that allowed Scheme I to describe the distributions of open and shut interval durations as well as theoretically possible. The fits to the distributions by Scheme I were the same as the continuous lines in *A* and *B*. In 81 additional minutes of simulated data, the predicted variation did not exceed that shown in *C*. Each point plots P_o calculated for 10 consecutive seconds of simulated channel activity. A comparison of predicted (*C*) to observed (Fig. 2 *C*) data indicates that Scheme I is insufficient to account for the wide range of P_o observed during wanderlust kinetics. The rate constants for Scheme I were (s^{-1}): 1–2 900.8; 1–4 1205; 2–1 33.02; 2–3 1709; 2–5 4977; 3–2 1735; 3–6 11.22; 4–1 13,560; 4–5 0.2924; 5–2 41,467; 5–4 0.007935; 5–6 354.6; 6–3 47.78; 6–5 184.1; 6–7 1348; 7–6 34.88; 7–8 224.3; 8–7 9.566; 8–9 26.11; 9–8 3.070; 9–10 1.558; 10–9 0.2884.

channels). The experimentally observed variability was considerably greater than that predicted by a simple model consistent with the dwell-time distributions. Thus, stochastic variation associated with a model like Scheme I cannot account for the observed variation in P_o.

Possible kinetic mechanisms for wanderlust kinetics

A possible mechanism for wanderlust kinetics is to assume that the channel switches slowly between high and low activity. To investigate this possibility, data obtained at the higher (>80%) and at the lower (<8.5%) levels of P_o for the experiment shown in Figs. 1 and 2 were collected and analyzed separately. The open and shut interval distributions at the higher levels of activity were described by the sums of two open and five shut exponential components (continuous lines through filled symbols, Fig. 6, *A* and *B*), whereas the open and shut interval distributions at the lower levels of activity were described by the sums of three open and six shut significant exponential components (continuous lines through open symbols, Fig. 6 *A* and *B*). Whereas many of the time constants describing the various exponential components differed between high and low activities, as indicated by differences in the positions of the peaks in Fig. 6, *A* and *B*, the major disparities were in the two longest shut components, which were 3–6 times more frequent and 15–25 times longer for the low activity than for the high.

In the four experiments analyzed in this manner, including the one presented in Fig. 6, the dwell-time distributions at the high levels of activity were described by two or three open and four or five shut exponential components, whereas the dwell-time distributions at the low levels of activity were described by two or three open and typically five or six shut exponential components. Differences in the estimated numbers of kinetic states at high and low activity could reflect actual differences, or the fact that it is often more difficult to detect closed states at high levels of activity because the time constants of the exponential components are less well separated than at lower levels of activity. Differences in the estimated numbers of kinetic states may

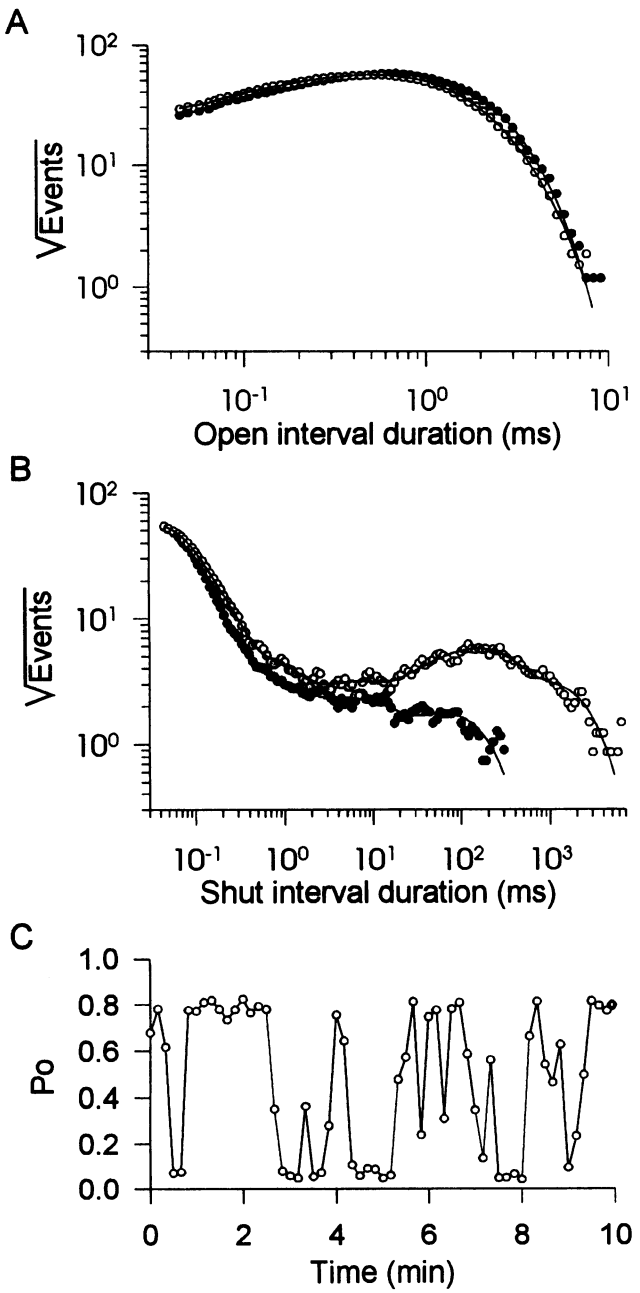

FIGURE 6 Characteristics of high and low channel activity during wanderlust kinetics. (*A* and *B*) Distributions of open and shut interval durations during periods of high (●) and low (○) activity for the experiment presented in Fig. 1 *A*. Regions of low ($P_o < 0.085$) and high ($P_o > 0.80$) activity were visually selected from Fig. 2 *B*, giving 56,000 and 137,000 intervals, respectively. The continuous lines are the fits to the distributions with sums of exponentials as described below. The distributions are normalized to 100,000 events for ease of comparison. The open intervals at high activity were described by the sum of two significant exponential components, with time constants and (areas) of 0.22 ms (0.061) and 0.66 ms (0.94). The open intervals at low activity were described by the sum of three significant exponentials: 0.13 ms (0.072), 0.48 ms (0.67), and 0.74 ms (0.26). The shut intervals at high activity were described by the sums of five significant exponential components: 0.027 ms (0.96), 0.091 ms (0.035), 0.59 ms (0.0027), 5.5 ms (0.0014), and 62 ms (0.00091). The shut intervals at low activity were described by the sums of six significant exponentials: 0.077 ms (0.107), 0.028 ms (0.87), 0.47 ms (0.0062), 4.2 ms (0.0021), 140 ms (0.0087), and 850 ms (0.0027). The distributions predicted by Scheme II with the rate constants in *C* for high and low activity considered separately were the same as the continuous lines. (*C*) Predicted variation in P_o as a function of time for Scheme II. The rate constants for the high and low activity modes of the Scheme were determined by fitting the high and low activity modes separately to the distributions shown in *A* and *B*. Each point plots the P_o calculated for 10 consecutive seconds of simulated channel activity. The rate constants for the low activity were (s^{-1}): 1–2 172.4; 1–4 1554; 2–1 67.01; 2–3 957.3; 2–5 5739; 3–2 5974; 3–6 50.14; 4–1 13,440; 4–5 0.02347; 5–2 40,561; 5–4 0.0746; 5–6 697.4; 6–3 49.53; 6–5 608.3; 6–7 1393; 7–6 112.4; 7–8 177.8; 8–7 39.25; 8–9 1.367; 9–8 1.478. The rate constants for the high activity were (s^{-1}): 1–2 3135; 1–3 720.0; 2–1 589.7; 2–4 4128; 3–1 11,240; 3–4 0.6572; 4–2 41,470; 4–3 0.07951; 4–5 184.8; 5–4 937.3; 5–6 674.5; 6–5 196.0; 6–7 65.98; 7–6 26.97. The rate constants connecting the high and low activity were (s^{-1}): 7(low)-6(high) 0.482; 6(high)-7(low) 1.463.

also reflect the fact that the data selected for analysis at the two levels of activity were not absolutely stable, because of the tendency of the channel to change P_o.

A specific model for wanderlust kinetics based on the experiment presented in Fig. 6 with five shut and two open components at high activity and six shut and three open components at low activity, then, might be described by Scheme II, which connects separate kinetic schemes for the two levels of activity with rate constants to give transition rates of about 0.1–0.01 s^{-1} between the two schemes so that the transitions between high and low activity occur, on average, about once every 10–100 s.

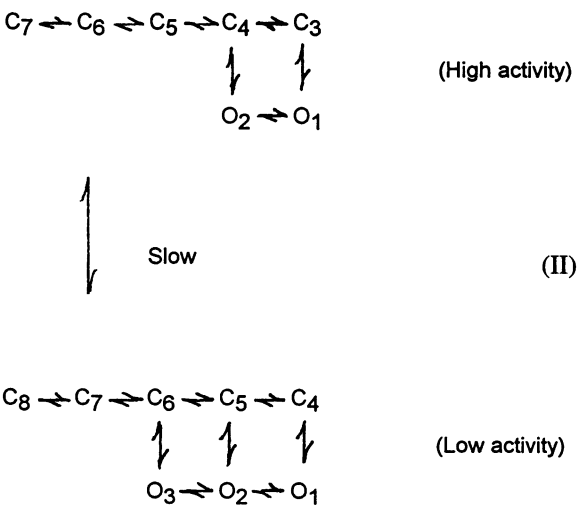

The continuous lines in Fig. 6, *A* and *B*, show that Scheme II can predict the dwell-time distributions during high and low activity, and the P_o plot in Fig. 6 *C* from the analysis of data simulated with Scheme II shows that this scheme can produce changes in P_o, the frequency and magnitude of which are similar to those observed experimentally (compare Fig. 6 *C* to Figs. 2 *C* and 3). Although Scheme II captured many of the features of wanderlust kinetics, it did not produce the slow creeping changes in activity that are observed in the experimental data, suggesting that Scheme II, with only two modes, is insufficient to describe wanderlust kinetics. Allowing rapid switching between the modes in Scheme II, with varying amounts of time spent in each mode, would be one method of producing intermediate levels of P_o to generate slow changes in activity. Another method would be to add additional modes to Scheme II. Adding such modes would be impractical, however, because of the large numbers of free parameters involved. Consequently, we explored the possibility that a single scheme with fixed rate constants, except for a multiplicative factor, could be used for each of the modes.

In developing this scheme we made the simplifying assumption that changes in P_o during wanderlust kinetics arise from apparent changes in the Ca^{2+}-dependent rate constants with time. The basis for this simplification comes from the observation that changes in P_o during wanderlust kinetics are associated with changes in the shut interval durations (Fig. 6 *B*) similar to the changes in shut interval durations produced by changing $Ca^{2+}{}_i$ (McManus and Magleby, 1991). To determine whether wanderlust kinetics might be described by apparent changes in the Ca^{2+}-dependent rate constants with time, we attempted to determine whether channel kinetics could be described by a model in which the rate constants were identical at low and high activities, except that the Ca^{2+} sensitivity of all the Ca^{2+}-dependent rate constants could change.

Scheme III, with three open and five closed states (the same as scheme X in McManus and Magleby, 1991), was used to simultaneously describe the gating at high and low levels of activity by solving for the rate constants and the apparent increase in the Ca^{2+}-dependent rate constants that gave the most likely descriptions of the dwell-time distributions at low and high activity. The continuous lines in Fig. 7, *A* and *B*, plot the predicted distributions, assuming that the change in P_o from low to high activity was equivalent to a 3.5-fold change in Ca^{2+} sensitivity of the Ca^{2+}-dependent rate constants. (Such an increase is functionally equivalent to multiplying the $Ca^{2+}{}_i$ by 3.5.)

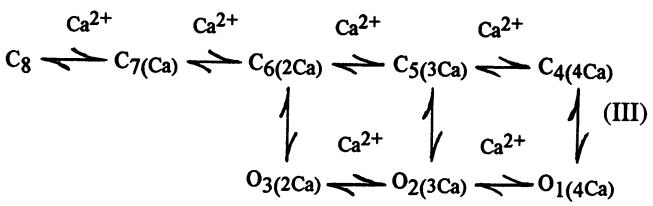

As shown in Fig. 7, *A* and *B*, the assumption of an apparent change in Ca^{2+} sensitivity could approximate the dwell-time distributions at high and low activity (Fig. 7, *A* and *B*), although the description was not as good as for Scheme II with all free parameters (Fig. 6, *A* and *B*). In four experiments of this type, the calculated increase in Ca^{2+}-dependent rate constants was 3.4 ± 0.7 from low to high activity.

Because Scheme III could approximate the high and low activity, the next step was to determine whether Scheme III could generate the other features of wanderlust kinetics. Because the results of Fig. 6 C indicated that transitions between two gating modes (Scheme II) were not sufficient to adequately describe the slow changes in activity, wanderlust kinetics was simulated with Scheme III assuming transitions among three gating modes. Each gating mode was described by Scheme III with identical rate constants, except for a multiplicative factor on the Ca^{2+}-dependent rate constants to give gating modes with low, medium, and high levels of P_o. Transitions among the gating modes were assumed to occur between the C6 states of Scheme III of the different modes, as indicated in the legend to Fig. 7.

The results of analyzing simulated currents generated with these assumptions are shown in Fig. 7 *C*. The predicted

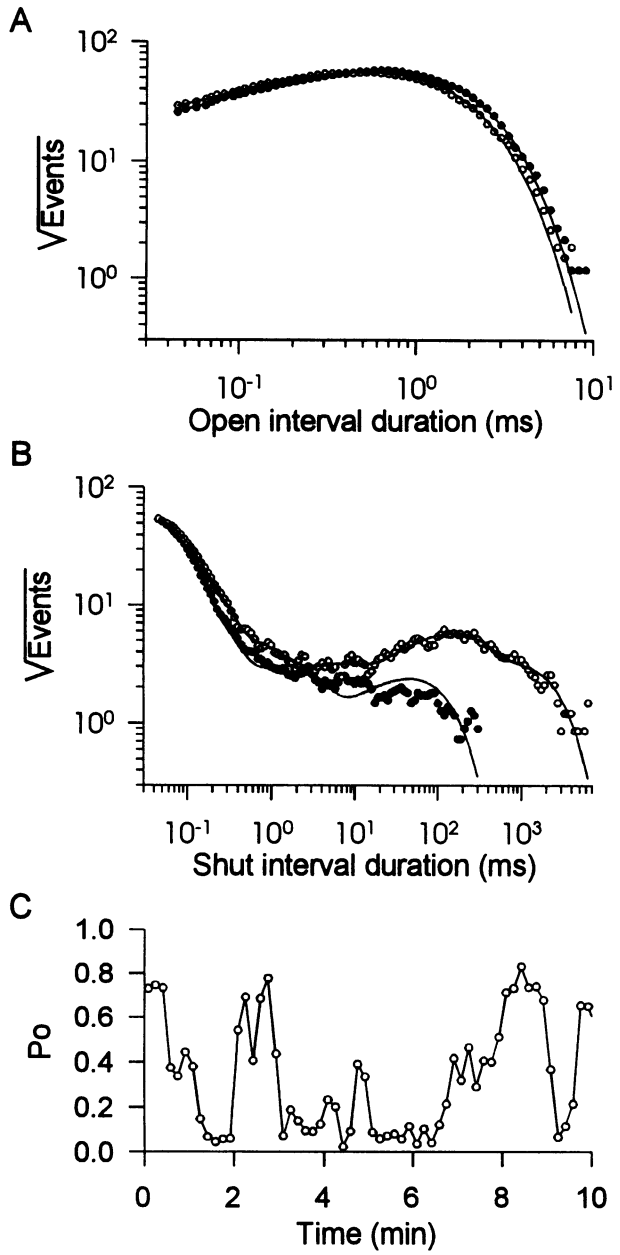

FIGURE 7 The distributions of interval durations at high and low activity can be approximated by assuming a change in the Ca^{2+}-dependent rate constants. (*A* and *B*) The distributions of interval durations at high (●) and low (○) activity from Fig. 6 were simultaneously fitted with Scheme III while allowing a different Ca^{2+} sensitivity for the Ca^{2+}-binding steps at the low activity. The continuous lines plot the predicted distributions. The Ca^{2+}-independent rate constants used for the predictions were (s^{-1}): 1–2 13,470; 1–4 2726; 2–3 0.1714; 2–5 3975; 3–6 5812; 4–1 62,163; 4–5 0.4393; 5–2 38,051; 5–6 103.0; 5–4 0.00904; 5–6 103.0; 6–3 8293; 6–7 1506; 7–8 281.4. The Ca^{2+}-dependent rate constants were (s^{-1}): 2–1 660.4; 3–2 1.360; 5–4 0.009045; 6–5 121.9; 7–6 76.17; 8–7 5.865. The Ca^{2+}-dependent rates were multiplied by 1.871 for the low activity and 6.5 for the high activity. (*C*) Predicted variation in P_o as a function of time for Scheme III, assuming that the channel made transitions among three modes, each described by Scheme III but with the Ca^{2+}-dependent rates multipled by 1.871 (mode 1), 3.8 (mode 2), and 6.5 (mode 3). Transitions between the three modes occurred in state C6. The rate constants for the transitions were (s^{-1}): C6(mode 1)-C6(mode 2) 15; C6(mode 2)-C6(mode 1) 4.73; C6(mode 2)-C6(mode 3) 4.73; C6(3)-C6(2) 6.53. Each point plots the P_o calculated for 10 consecutive seconds of simulated channel activity.

properties of wanderlust kinetics were similar to the observed properties, including the slow changes between different levels of P_o (compare Fig. 7 *C* to Figs. 2 *C* and 3).

DISCUSSION

The recent isolation of complementary DNAs encoding large conductance Ca^{2+}-activated K^+ channels provides a means of studying the kinetic gating properties of BK channels with known primary structure (Atkinson et al., 1991; Adelman et al., 1992; Butler et al., 1993; Lagrutta et al., 1994; Pallanck and Ganetzky, 1994; Tseng-Crank et al., 1994; Wei et al., 1994). Analysis of currents recorded from cloned *dSlo* channels expressed in *Xenopus* oocytes has led to two main observations in this study: 1) the Ca^{2+} sensitivity, as measured by the $[Ca^{2+}]_i$ required for a P_o of 0.5, varied by as much as threefold among different channels from the same clone; and 2) individual channels typically exhibited slow fluctuating changes in P_o (wanderlust kinetics) that were considerably greater than the stochastic variation expected for gating models consistent with native BK channel activity.

Differences in Ca^{2+} sensitivity among cloned channels

The observation of differences in Ca^{2+} sensitivity among cloned channels is similar to differences in $Ca^{2+}{}_i$ sensitivity among native BK channels from cultured rat skeletal muscle (McManus and Magleby, 1991) and avian salt glands (Wu et al., 1996), and for sustained shifts in Ca^{2+} sensitivity for single native BK channels in smooth muscle (Singer and Walsh, 1987). A possible explanation for the differences among native channels is that the α-subunit composition among native channels may differ because of natural variants arising from alternative splicing (Adelman et al., 1992; Butler et al., 1993; Pallanck and Ganetzky, 1994; Tseng-Crank et al., 1994). Specific areas in the C-terminal domain of *dSlo* that are alternatively spliced can alter Ca^{2+} sensitivity (Lagrutta et al., 1994). Our observation that differences in Ca^{2+} sensitivity persist among cloned channels does not rule out natural variants as an explanation for differences in Ca^{2+} sensitivity that persist in native channels, but it does suggest that alternative splicing is not necessary to obtain such differences in Ca^{2+} sensitivity. Consistent with our observation of heterogeneous properties among cloned channels expressed in *Xenopus* oocytes, cloned nicotinic acetylcholine receptors expressed in *Xenopus* oocytes also show heterogeneous properties (Gibb et al., 1990).

Wanderlust kinetics differs from typical mode shifting in native BK channels

Mode shifting among different types of gating is a common feature of ion channel kinetics (Patlak et al., 1979;

Siegelbaum et al., 1982; Hess et al., 1984; Auerbach and Lingle, 1986; Patlak et al., 1986; Naranjo and Brehm, 1993), including native BK channels (Moczydlowski and Latorre, 1983; McManus and Magleby, 1988). Wanderlust kinetics differs from typical mode shifting in native BK channels in that typical mode shifting appears to occur instantaneously between two well-defined types of kinetic activity, whereas wanderlust kinetics occurs more slowly between changing levels of P_o (Figs. 1 and 3).

Another difference between wanderlust kinetics and typical mode shifting is that wanderlust kinetics is associated mainly with changes in the mean shut time (Fig. 2), whereas typical mode shifting in native BK channels is associated with large changes in mean open time as well as mean shut time (McManus and Magleby, 1988). The limited effect of wanderlust kinetics on the mean open time may be related to the observation that the mean open time for *dSlo* channels expressed in oocytes is less sensitive to $Ca^{2+}{}_i$ than the mean open time of native BK channels (Silberberg and Magleby, unpublished observations). Because of the wanderlust kinetics and changing P_o, it would be difficult to define a dominant or normal mode of activity for the cloned BK channels. In contrast, native BK channels typically spend 96–97% of their time in normal (nonmoding) stable activity (McManus and Magleby, 1988), and if there are changes in activity, they are usually preceded and followed by stable periods (Singer and Walsh, 1987).

Gating kinetics for wanderlust kinetics

The gating of native BK channels is consistent with a discrete Markov gating process, with the transition rates among discrete states of the channel remaining constant in time for constant conditions (McManus and Magleby, 1989). We found that the slow changes in kinetics associated with wanderlust kinetics could also be generated by a discrete-state Markov model, provided that the model allowed transitions among three gating modes with low, medium, and high P_o (Fig. 7 *C*). Each gating mode was described by Scheme III with identical rate constants, except for a multiplicative factor that acted on the Ca^{2+}-dependent rate constants. If necessary, additional gating modes giving additional levels of P_o could be added to generate even slower processes, as additional modes might be expected (see below).

Although it was possible to generate apparent slow changes in kinetics with Markov gating, we have not excluded the possibility that wanderlust kinetics could be related to changes in rate constants that depend directly on the previous gating history of the channel. Such memory-dependent changes in rate constants would indicate non-Markov gating.

Possible mechanisms

The mechanisms underlying wanderlust kinetics and differences in $Ca^{2+}{}_i$ sensitivity are not clear, but could be related to changes in the environment of the channels or to changes in the subunits of the channels. These possibilities will be considered in order.

Xenopus oocytes have internal calcium stores that reside close to the plasma membrane (Gardiner and Grey, 1983). If these stores remain attached to the intracellular aspect of the patch and undergo periodic release of Ca^{2+}, then this might give rise to wanderlust kinetics. Such periodic release of Ca^{2+} can give rise to variable kinetics for BK channels in excised patches from smooth muscle (Xiong et al., 1992). Periodic release of Ca^{2+} seems unlikely, however, as an explanation for wanderlust kinetics in our experiments. Agents that should have emptied internal Ca^{2+} stores (caffeine, thapsigargin) or increased the Ca^{2+} buffering capacity (HEDTA) had little apparent effect on wanderlust kinetics. We have not ruled out, however, that wanderlust kinetics might arise in some manner from thapsigargin and caffeine resistant Ca^{2+} stores of the type found in growth cones (Gomez et al., 1995).

Differences in membrane fluidity (Moczdlowski et al., 1985) and phospholipid composition (Bregestovski and Bolotina, 1989; Bolotina et al., 1989) can alter apparent Ca^{2+} sensitivity and channel activity. However, we are not aware of evidence suggesting that either membrane parameter could fluctuate in excised patches to produce wanderlust kinetics or be stable and different for different channels to produce variable Ca^{2+} sensitivity among channels.

If wanderlust kinetics or differences in Ca^{2+} sensitivity arise from specific changes in the channel rather than the environment, then the homotetrameric structure of the cloned channel (Shen et al., 1994) suggests some possible mechanisms.

If each one of the four subunits can be in, for example, a low- or high-activity form, then there might be up to six different levels (or modes) of channel activity arising from the six possible combinations of subunits shown in Fig. 8. If the subunits switched back and fourth asychronously at a low rate between the high- and low-activity forms during an experiment, then the changing combinations of different forms of subunits could lead to wanderlust kinetics. Alternatively, if each subunit retained its particular activity form throughout an experiment, then this could yield different levels of maintained Ca^{2+} sensitivity. Some support for the latter possibility comes from the observations of Wu et al. (1996) that the Ca^{2+} sensitivity of BK channels from the avian nasal salt gland can be grouped into five clusters, consistent with a model in which the random mixing of two

FIGURE 8 If each subunit of a tetrameric channel can be in a high or low activity form, then there are six possible combinations of subunits. If a channel with two diagonal subunits in the same form has the same properties as one with two adjacent subunits in the same form, then there would be five functional types of channel.

different types of subunits, with either high or low Ca^{2+} sensitivity, gives rise to the differences in Ca^{2+} sensitivity.

A number of factors known to modulate channel activity could be potential candidates for changing the activity form of the subunits. Changes in phosphorylation can alter the Ca^{2+} sensitivity of channels, leading to changes in P_o at a constant $[Ca^{2+}]_i$ (De Peyer et al., 1982; Reinhart et al., 1991; White et al., 1991; Bielefeldt and Jackson, 1994; Esguerra et al., 1994). If such changes in phosphorylation occurred slowly and reversibly over time, then this might lead to wanderlust kinetics. Such a mechanism for wanderlust kinetics seems unlikely, however, because there would have to be sufficient intrinsic energy stores in the perfused excised patches for 20–100 phosphorylation-deposphorylation cycles to account for the continual fluctuation in P_o over the course of the experiments.

Alternatively, if some BK channels had stable levels of phosphorylation that differed from other BK channels, then this could provide a basis for the differences in Ca^{2+} sensitivity among channels. If differences in phosphorylation are the explanation for differences in Ca^{2+} sensitivity, then channels in the excised patches would have to retain stable levels of phosphorylation for extended periods of time, as the mean activity of the channels could remain stable for many tens of minutes. We found that eliminating a putative phosphorylation site for cAMP-dependent protein kinase (PKA) by mutating a serine at site 942 to an alanine (S942A) did not eliminate either wanderlust kinetics or differences in Ca^{2+} sensitivity among channels. This observation does not rule out the possibility that these two phenomena may reflect changes in phosphorylation, however, because phosphorylation may occur at other sites on the channel.

Actin filaments can alter Na^+, Ca^{2+}, N-methyl-D-aspartate, and Cl^- channel activity (Cantiello et al., 1991; Johnson and Byerly, 1993; Rosenmund and Westbrook, 1993; Suzuki et al., 1993). It will require further investigation to determine whether maintained or changing differences in cytoskeletal associations with one or more subunits of BK channels contributes to differences in Ca^{2+} sensitivity or wanderlust kinetics.

Some native BK channels are composed of at least two types of subunits, α and β, with the addition of the modulatory β-subunits conferring a tenfold increase in Ca^{2+} sensitivity (Garcia-Calvo et al., 1994; McManus et al., 1995). Only the message for α-subunits was injected in the oocytes for the experiments in this paper. It is not yet known whether *dSlo* channels are normally associated with β-subunits (or other accessory proteins), or whether there might be endogenous β-like subunits in the oocyte. If endogenous β-like subunits were present, then association of a variable number of endogenous β-like subunits with the expressed channel could give rise to wanderlust kinetics or differences in Ca^{2+} sensitivity, depending on whether the number of associated β-like subunits changed during an experiment or remained stable.

If the *Xenopus* oocytes expressed endogenous BK channels or endogenous α-subunits that coassembled with the α-subunits from *dSlo*, then different types of channels with different Ca^{2+} sensitivities might be produced. Although we have not observed endogenous BK channels in uninjected *Xenopus* oocytes in 21 patches in which other types of endogenous channels were present to verify that the patch was functional, the possibility of endogenous BK channels cannot be ruled out.

Because the expressed cloned BK channels typically displayed both wanderlust kinetics and differences in Ca^{2+} sensitivity, some combination of factors would be required to account for both of these phenomena.

We thank Dr. Gerhard Dahl and Audrey Llanes for their assistance with the preparation and injection of oocytes for many of the experiments.

Supported by grants AR32805 (KLM) and NS31872 (JPA) from the National Institutes of Health, a grant from the Muscular Dystrophy Association (KLM), and grants 93-00061 from the US-Israel Binational Science Foundation and 6247194 from the Israeli Ministry of Science and the Arts (SDS).

REFERENCES

Adams, P. R., A. Constanti, D. A. Brown, and R. B. Clark. 1982. Intracellular Ca^{2+} activates a fast voltage-sensitive K^+ current in vertebrate sympathetic neurones. *Nature.* 296:746–749.

Adelman, J. P., K. Z. Shen, M. P. Kavanaugh, R. A. Warren, Y. N. Wu, A. Lagrutta, C. T. Bond, and R. A. North. 1992. Calcium-activated potassium channels expressed from cloned complementary DNAs. *Neuron.* 9:209–216.

Atkinson, N. S., G. A. Robertson, and B. Ganetzky. 1991. A component of calcium-activated potassium channels encoded by the Drosophila slo locus. *Science.* 253:551–555.

Auerbach, A., and C. J. Lingle. 1986. Heterogeneous kinetic properties of acetylcholine receptor channels in Xenopus myocytes. *J. Physiol. (Lond.).* 378:119–140.

Barrett, J. N., K. L. Magleby, and B. S. Pallotta. 1982. Properties of single calcium-activated potassium channels in cultured rat muscle. *J. Physiol. (Lond.).* 331:211–230.

Bielefeldt, K., and M. B. Jackson. 1994. Phosphorylation and dephosphorylation modulate a Ca^{2+}-activated K^+ channel in rat peptidergic nerve terminals. *J. Physiol. (Lond.).* 475:241–254.

Blatz, A. L., and K. L. Magleby. 1986a. Correcting single channel data for missed events. *Biophys. J.* 49:967–980.

Blatz, A. L., and K. L. Magleby. 1986b. Quantitative description of three modes of activity of fast chloride channels from rat skeletal muscle. *J. Physiol. (Lond.).* 378:141–174.

Bolotina, V., V. Omelyanenko, B. Heyes, U. Ryan, and P. Bregestovski. 1989. Variations of membrane cholesterol alter the kinetics of Ca^{2+}-dependent K^+ channels and membrane fluidity in vascular smooth muscle cells. *Pflugers Arch. Eur. J. Physiol.* 415:262–268.

Bregestovski, P. D., and V. N. Bolotina. 1989. Membrane fluidity and kinetics of Ca^{2+}-dependent potassium channels. *Biomed. Biochim. Acta.* 48:S382–S387.

Butler, A., S. Tsunoda, D. P. McCobb, A. Wei, and L. Salkoff. 1993. mSlo, a complex mouse gene encoding "maxi" calcium-activated potassium channels. *Science.* 261:221–224.

Cantiello, H. F., J. L. Stow, A. G. Prat, and D. A. Ausiello. 1991. Actin filaments regulate epithelial Na^+ channel activity. *Am. J. Physiol.* 261: C882–C888.

Clapham, D. E. 1995. Calcium signaling. *Cell.* 80:259–268.

Colquhoun, D., and F. J. Sigworth. 1995. Fitting and statistical analysis of single-channel records. *In* Single-Channel Recording. B. Sakmann and E. Neher, editors. Plenum Press, New York. 483–587.

Dahl, G. 1992. The oocyte cell-cell channel assay for functional analysis of gap junction proteins. *In* Cell-Cell Interactions: A Practical Approach. B. Stevenson, D. Paul, and W. Gallin, editors. Oxford University Press, London and New York. 143–165.

De Peyer, J. E., A. B. Cachelin, I. B. Levitan, and H. Reuter. 1982. Ca^{2+}-activated K^+ conductance in internally perfused snail neurons is enhanced by protein phosphorylation. *Proc. Natl. Acad. Sci. USA.* 79:4207–4211.

Esguerra, M., J. Wang, C. D. Foster, J. P. Adelman, R. A. North, and I. B. Levitan. 1994. Cloned Ca^{2+}-dependent K^+ channel modulated by a functionally associated protein kinase. *Nature.* 369:563–565.

Farley, J., and B. Rudy. 1988. Multiple types of voltage-dependent Ca^{2+}-activated K^+ channels of large conductance in rat brain synaptosomal membranes. *Biophys. J.* 53:919–934.

Garcia-Calvo, M., H. G. Knaus, O. B. McManus, K. M. Giangiacomo, G. J. Kaczorowski, and M. L. Garcia. 1994. Purification and reconstitution of the high-conductance, calcium-activated potassium channel from tracheal smooth muscle. *J. Biol. Chem.* 269:676–682.

Gardiner, D. M., and R. D. Grey. 1983. Membrane junctions in *Xenopus* eggs: their distribution suggests a role in calcium regulation. *J. Cell Biol.* 96:1159–1163.

Gibb, A. J., H. Kojima, J. A. Carr, and D. Colquhoun. 1990. Expression of cloned receptor subunits produces multiple receptors. *Proc. R. Soc. Lond. B.* 242:108–112.

Gomez, T. M., D. M. Snow, and P. C. Letourneau. 1995. Characterization of spontaneous calcium transients in nerve growth cones and their effect on growth cone migration. *Neuron.* 14:1233–1246.

Hamill, O. P., A. Marty, E. Neher, B. Sakmann, and F. J. Sigworth. 1981. Improved patch clamp techniques for high-resolution current recording from cells and cell-free membrane patches. *Pflugers Arch. Eur. J. Physiol.* 391:85–100.

Hess, P., J. B. Lansman, and R. W. Tsien. 1984. Different modes of Ca channel gating behaviour favoured by dihydropyridine Ca agonists and antagonists. *Nature.* 311:538–544.

Johnson, B. D., and L. Byerly. 1993. A cytoskeletal mechanism for Ca^{2+} channel metabolic dependence and inactivation by intracellular Ca^{2+}. *Neuron.* 10:797–804.

Lagrutta, A., K. Shen, R. A. North, and J. P. Adelman. 1994. Functional differences among alternatively spliced variants of *slowpoke*, a *Drosophila* calcium-activated potassium channel. *J. Biol. Chem.* 269: 20347–20351.

Latorre, R., A. Oberhauser, P. Labarca, and O. Alvarez. 1989. Varieties of calcium-activated potassium channels. *Annu. Rev. Physiol.* 51:385–399.

Latorre, R., C. Vergara, and C. Hidalgo. 1982. Reconstitution in planar lipid bilayers of a Ca^{2+}-dependent K^+ channel from transverse tubule membranes isolated from rabbit skeletal muscle. *Proc. Natl. Acad. Sci. USA.* 79:805–809.

Marty, A. 1981. Ca-dependent K channels with large unitary conductance in chromaffin cell membranes. *Nature.* 291:497–500.

McManus, O. B., A. L. Blatz, and K. L. Magleby. 1987. Sampling, log binning, fitting, and plotting durations of open and shut intervals from single channels and the effects of noise. *Pflugers Arch. Eur. J. Physiol.* 410:530–553.

McManus, O. B., L. M. H. Helms, L. Pallanck, B. Ganetzky, R. Swanson, and R. J. Leonard. 1995. Functional role of the beta subunit of high-conductance calcium-activated potassium channels. *Neuron.* 14: 645–650.

McManus, O. B., and K. L. Magleby. 1988. Kinetic states and modes of single large-conductance calcium-activated potassium channels in cultured rat skeletal muscle. *J. Physiol. (Lond.).* 402:79–120.

McManus, O. B., and K. L. Magleby. 1989. Kinetic time constants independent of previous single-channel activity suggest Markov gating for a large conductance Ca-activated K channel. *J. Gen. Physiol.* 94:1037–1070.

McManus, O. B., and K. L. Magleby. 1991. Accounting for the Ca^{2+}-dependent kinetics of single large-conductance Ca^{2+}-activated K^+ channels in rat skeletal muscle. *J. Physiol. (Lond.).* 443:739–777.

Moczydlowski, E., O. Alvarez, C. Vergara, and R. Latorre. 1985. Effect of phospholipid surface charge on the conductance and gating of a Ca^{2+}-activated K^+ channel in planar lipid bilayers. *J. Membr. Biol.* 83:273–282.

Moczydlowski, E., and R. Latorre. 1983. Gating kinetics of Ca^{2+}-activated K^+ channels from rat muscle incorporated into planar lipid bilayers. Evidence for two voltage-dependent Ca^{2+} binding reactions. *J. Gen. Physiol.* 82:511–542.

Naranjo, D., and P. Brehm. 1993. Modal shifts in acetylcholine receptor channel gating confer subunit-dependent desensitization. *Science.* 260: 1811–1814.

Pallanck, L., and B. Ganetzky. 1994. Cloning and characterization of human and mouse homologs of the Drosophila calcium-activated potassium channel gene, slowpoke. *Hum. Mol. Genet.* 3:1239–1243.

Pallotta, B. S., K. L. Magleby, and J. N. Barrett. 1981. Single channel recordings of Ca^{2+}-activated K^+ currents in rat muscle cell culture. *Nature.* 293:471–474.

Patlak, J. B., K. A. F. Gration, and P. N. R. Usherwood. 1979. Single glutamate-activated channels in locust muscle. *Nature.* 278:643–645.

Patlak, J. B., M. Ortiz, and R. Horn. 1986. Opentime heterogeneity during bursting of sodium channels in frog skeletal muscle. *Biophys. J.* 49: 773–777.

Poledna, J., and V. Packova. 1994. Caffeine suppresses chloride current fluctuations in calcium-overloaded *Xenopus laevis* oocytes. *Physiol. Res.* 43:253–256.

Reinhart, P. H., S. Chung, B. L. Martin, D. L. Brautigan, and I. B. Levitan. 1991. Modulation of calcium-activated potassium channels from rat brain by protein kinase A and phosphatase 2A. *J. Neurosci.* 11:1627–1635.

Rosenmund, C., and G. L. Westbrook. 1993. Calcium-induced actin depolymerization reduces NMDA channel activity. *Neuron.* 10:805–814.

Rousseau, E., J. Ladine, Q. Y. Liu, and G. Meissner. 1988. Activation of the Ca^{2+} release channel of skeletal muscle sarcoplasmic reticulum by caffeine and related compounds. *Arch. Biochem. Biophys.* 267:75–86.

Rudy, B. 1988. Diversity and ubiquity of K channels. *Neuroscience.* 25:729–749.

Sakmann, B., and E. Neher. 1995. Single-Channel Recording. Plenum Publishing, New York.

Shen, K.-Z., A. Lagrutta, N. W. Davies, N. B. Standen, J. P. Adelman, and R. A. North. 1994. Tetraethylammonium block of *slowpoke* calcium-activated potassium channels expressed in *Xenopus* oocytes: evidence for tetrameric channel formation. *Pflugers Arch. Eur. J. Physiol.* 426:440–445.

Siegelbaum, S. A., J. S. Camardo, and E. R. Kandel. 1982. Seratonin and cyclic AMP close single K^+ channels in *Aplysia* sensory neurones. *Nature.* 299:413–417.

Sigworth, F. J., and S. M. Sine. 1987. Data transformations for improved display and fitting of single-channel dwell time histograms. *Biophys. J.* 52:1047–1054.

Silberberg, S. D., A. Lagnutta, J. P. Adelman, and K. L. Magleby. 1995. Slow gating processes can modulate activity of a cloned Ca^{2+}-activated K^+ (BK) channel. *Biophys. J.* 68:A3.

Singer, J. J., and J. V. Walsh, Jr. 1987. Characterization of calcium-activated potassium channels in single smooth muscle cells using the patch-clamp technique. *Pflugers Arch. Eur. J. Physiol.* 408:98–111.

Suzuki, M., K. Miyazaki, M. Ikeda, Y. Kawaguchi, and O. Sakai. 1993. F-actin network may regulate a Cl- channel in renal proximal tubule cells. *J. Membr. Biol.* 134:31–39.

Tseng-Crank, J., C. D. Foster, J. D. Krause, R. Mertz, N. Godinot, T. J. DiChiara, and P. H. Reinhart. 1994. Cloning, expression, and distribution of functionally distinct Ca^{2+}-activated K^+ channel isoforms from human brain. *Neuron.* 13:1315–1330.

Wei, A., C. Solaro, C. Lingle, and L. Salkoff. 1994. Calcium sensitivity of BK-type K_{Ca} channels determined by a separable domain. *Neuron.* 13:671–680.

White, R. E., A. Schonbrunn, and D. L. Armstrong. 1991. Somatostatin stimulates Ca^{2+}-activated K^+ channels through protein dephosphorylation. *Nature.* 351:570–573.

Wu, J. V., T. J. Trevor, and P. Stampe. 1996. Grouped calcium titration curves: gating components of the calcium-activated K^+ channels may be heterotetramerous. *Biophys. J.* 70:A192.

Xiong, Z. L., K. Kitamura, and H. Kuriyama. 1992. Evidence for contribution of Ca^{2+} storage sites on unitary K^+ channel currents in inside-out membrane of rabbit portal vein. *Pflugers Arch. Eur. J. Physiol.* 420: 112–114.